TWIN-SLOT ANTENNA COUPLED NB HOT ELECTRON BOLOMETER MIXERS AT 1 THZ AND 2.5 THZ

W.F.M. Ganzevles[†1], J.R. Gao[‡], D. Wilms Floet[†], G. de Lange[‡], A.K. van Langen[†], L.R. Swart[§], T.M. Klapwijk[†] and P.A.J. de Korte[‡]

[†]Department of Applied Physics
Delft University of Technology
Lorentzweg 1, 2628 CJ Delft, The Netherlands

[‡]Space Research Organization of the Netherlands
PO Box 800, 9700 AV Groningen, The Netherlands

[§]Department of Applied Physics
University of Groningen
Nijenborgh 4, 9747 AG Groningen, The Netherlands

Abstract

We have designed quasi-optically coupled Nb diffusion-cooled Hot Electron Bolometer Mixers (DC HEBMs) using a twin-slot antenna and Co-Planar Waveguide (CPW) transmission lines for 1.0 and 2.5 THz. The devices have been realized using two-step e-beam lithography and deep UV lithography. DC measurements give a critical temperature of the bridge of 6.1 K and a critical current density of $7 \times 10^{10} \mathrm{Am}^{-2}$. Typical normal state values for R_{square} are in the order of 30Ω. At 1 THz, we obtain, in contrast to results at 2.5 THz, excellent agreement between design and the response as measured in a Fourier Transform Spectrometer. For the 2.5 THz devices the peak response is shifted to 1.5 THz, similar to results reported in literature[1]. Heterodyne measurements on a 1 THz mixer have shown a corrected receiver noise temperature $T_{N,corr}$ of 3600 K at $T_{bath} = 3.3$K. The Y-factor measurements at different IF suggest an IF bandwidth of at least 1.7 GHz.

[1]Corresponding address:
Department of Applied Physics
University of Groningen
Nijenborgh 4, 9747 AG Groningen, The Netherlands
electronic mail: W.F.M.Ganzevles@phys.rug.nl

1 Introduction

The recent interest in the investigation of the universe through one of the last major windows of the electromagnetic spectrum has given large impetus to research and development of sub-millimeter detectors.

Up to about 1 THz, Nb superconductor-insulator-superconductor (SIS) mixers have proven to be very suitable. Above this frequency, superconducting Hot Electron Bolometer Mixers (HEBMs) are promising candidates to fulfill the need for low-noise, high frequency detectors.

In order to study diffusion-cooled Nb HEBMs at high frequencies, we develop an RF setup using Quasi-Optical (QO) techniques to couple radiation to the microbridge. Our design includes lens, holder, on-chip RF and IF structures and the connection to the IF chain.

In this contribution, we will describe our on-chip RF design and the device fabrication process. DC measurements are reported and we will describe the design of some major components used in our receiver. Predicted RF response is then compared to the measured response around both 1 THz and 2.5 THz as considerable disagreement exists between calculation and measurements of the response. This is observed by both Karasik et al.[1] and the authors. Lastly, we report heterodyne measurements at 0.93 THz.

2 RF design and characterization

Out of a number of possible antenna geometries such as log periodic, log spiral and double dipole, we have chosen the twin slot antenna because it has properties suitable to possible applications. Among these, there are reasonably small bandwidth, linear polarization, circular beam pattern, good Gaussian coupling and low sidelobe levels.

The antenna geometry we use has length $l = 0.32\lambda_0$, separation $s = 0.16\lambda_0$ and width $w = 0.05 \cdot l$, where λ_0 is the free-space wavelength. Several antennas close to this geometry have been investigated. We have chosen this particular geometry because it has almost zero imaginary part at the center frequency f_{center} and a reasonably symmetric beam pattern.

To feed the signal to the heart of the detector, a superconducting Nb bridge with a length, width and thickness of typically 200 nm × 200 nm × 12 nm, we use a Co-Planar Waveguide (CPW) transmission line. This line has nominal dimensions slot width $a = 0.5\mu$m and center line width $b = 2\mu$m.

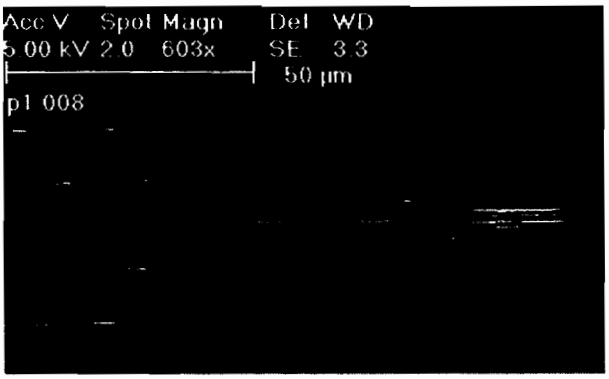

Figure 1: *Lay out of a 2.5 THz device. The antenna and filter are clearly visible, as is the IF CPW on the left. The GPW transmission lines connect the antenna to the bridge.*

A $\frac{1}{4}\lambda$ RF filter is used to prevent signal from entering the IF chain. The filter consists of high impedance sections with a width of 1.5 μm and low impedance sections having a width of 8 μm. At 2.5 THz, the length of the sections is 12 μm. A CPW transmission line is connected to the filter. This acts as the connection to both the DC bias supply and the IF amplifier. Fig. 1 shows an SEM micrograph of a 2.5 THz device. A similar design is reported in literature at various frequencies[1],[2].

To design the RF structure to be used in the QO HEBMs, we use a method in which we separate the antenna, filter and CPW transmission line to obtain the coupling efficiency of the antenna-bridge combination. The impedance of each of these elements is calculated separately, using analytical formulas from [3]. The antenna impedance however is calculated using a computer program by Zmuidzinas and Chattopadhyay[4], based on a model by Kominami et al.[5]. We only include geometry and ε_r of the structure.

For small CPW-structures, we find that the models from[3] yield results that are doubtfull[6]. Therefore, we use several commercially available software programs ([7],[8]), yielding $Z_{0,\mathrm{CPW}} = 39\,\Omega$. This value then is linearly extrapolated using the CPW geometry as measured after device fabrication. The impedance of each filter section is calculated using a model from [3], as the filter is relatively large and both [3] and [7],[8] yield similar results. In this paper, we will call this approach the analytical approach, although not fully justified.

For the HEB impedance Z_{HEB}, we assume the normal state resistance of

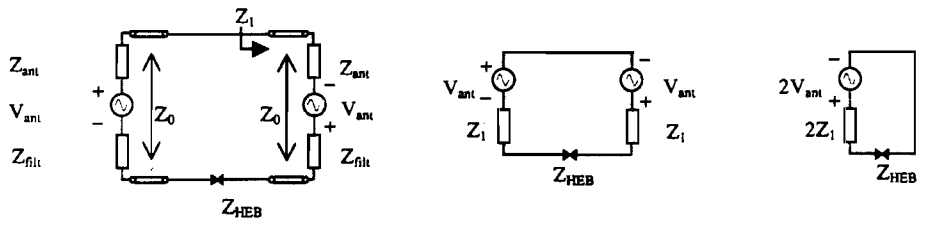

Figure 2: *Equivalent circuit used in the analytical RF modeling.*

the device R_N. Using the equivalent circuit shown in Fig. 2 (which is similar to the one in [2]), we then calculate the coupling efficiency η between the HEB and the antenna-filter-loaded CPW, having total impedance Z_1, using the relation

$$\eta = \frac{4Re\,(Z_{HEB})\,Re\,(Z_1)}{|Z_{HEB} + Z_1|^2}, \tag{1}$$

where Z_1 is the effective impedance seen by the bolometer. Results will be presented in section 5.2. Note that in this approach, the disturbing influence of the filter on the antenna geometry is not taken into account. Only reflection losses are taken into account.

3 Device Fabrication

A fabrication process for Nb HEBMs has been developed using two-step electron beam lithography (EBL) to define both bridge length and width. Deep UV lithography is used to define the RF structure. In this section, we shortly sketch the fabrication process of the device. DC measurements will be shown in section 4, indicating that this process is suitable for production of diffusion cooled QO HEBMs.

In the first step, 75 nm thick Au squares are DC-magnetron sputtered on the high-resistivity Si substrate (double-sided polished). These are used as alignment markers in subsequent optical and e-beam lithography steps.

Then we deposit 12 nm Nb using magnetron sputtering. Using a lift-off mask, only patches 12 μm $\times$12 μm are covered. This decreases the amount of Nb to be opened up for etching, thus reducing the writing area in the EBL machine. Also, only a small fraction of RF current has to run in –lossy– Nb. Au coolpads (100 nm thick) are defined using EBL in a double layer

PMMA system. RF cleaning of the Nb in an Ar-plasma is used to remove the native Nb oxide, in order to achieve a high interface transparency. In situ, ~ 10 nm Au is sputtered. Then, 90 nm Au is e-beam evaporated at a pressure of 2×10^{-6}mbar.

After lift-off, 5 nm Al plus 10 nm Au is sputtered, using a lift-off mask in Shipley DUV III-resist. This layer requires the use of DUV lithography because of the 0.5 μm slots in the CPW structure. 160 nm Au is evaporated under similar conditions as the cooling pads. As a last optical step, we deposit 100 nm Nb on the IF CPW-transmission line.

In the last production step, we define the bridge width. Using EBL, we define a PMMA bridge in the double layer resist system as before. Only the Nb parts that have to be etched are opened up, see Fig. 3. In a mixture of CF_4+3%O_2, the Nb is reactive ion etched. We monitor the process by measuring the optical reflectivity of the Nb on the Si substrate by using a laser endpoint detection system. Using this process we are able to produce Nb bridges as small as 60 nm, as shown in Fig. 3.

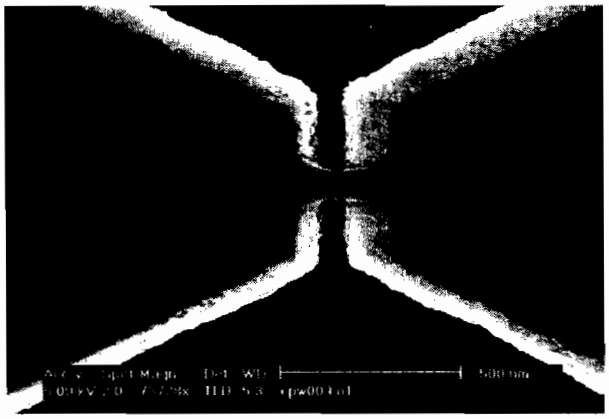

Figure 3: *The microbridge after etching. The PMMA etch mask is still present. Bridge dimensions: $l \times w \sim 60$ nm$\times 80$ nm. The tapered structures are the Au cooling pads.*

During processing, all devices are electrically shorted. After dicing these shorts are opened. Therefore, all further handling must be done with extreme care to prevent damage due to electrostatic discharge. After wire bonding, DC measurements are performed at 4.2 K in a metal vacuum can.

4 DC Measurements

Suitable devices for RF measurements are selected based on IV-curves. Also the R-T curve is used for quality assessment. Several devices show IV-curves that are suitable for use in RF experiments.

Measurements on a large structure yield for 12 nm Nb a residual resistance ratio (RRR) of 1.65 and a square resistance of about $R_{square} = 33\Omega$. The gold, 175 nm thick, that is used for the RF structure has an RRR of around 3.5 and $R_{square} = 0.1\Omega$.

As can be seen in Fig. 4, the critical temperature of the Nb bridge $T_{c,bridge}$ is 6.1 K. The Nb under the cooling pads $T_{c,pads}$ is 5.2 K. Both values are close to what is found in literature[1],[9],[10].

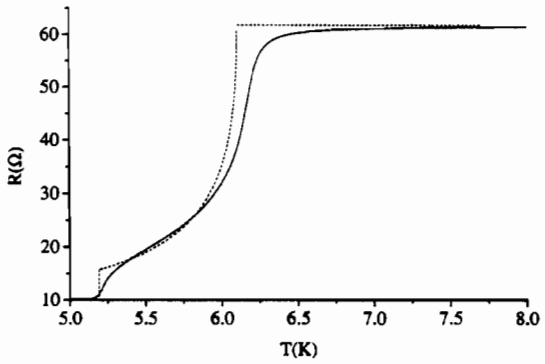

Figure 4: *RT-curve of 1 THz device. The simulation (dashed) is done assuming* $T_{c,bridge} = 6.1$ K; $R_{square} = 33\Omega$.

The RT-curve is modelled according to [11] (dashed line in Fig. 4), taking into account the superconducting proximity effect, Andreev reflection and charge imbalance. The measured curve can be modelled reasonably well. This indicates that our devices show RT-behavior as one would expect.

An unpumped IV-curve of a bridge (nominally 200 nm long, 200 nm wide, 12 nm thick) is shown in Fig. 8 (dashed line). We observe a critical current density of 7×10^{10} Am^{-2}. This agrees to values found in literature[1],[9],[12] within a factor of 2.

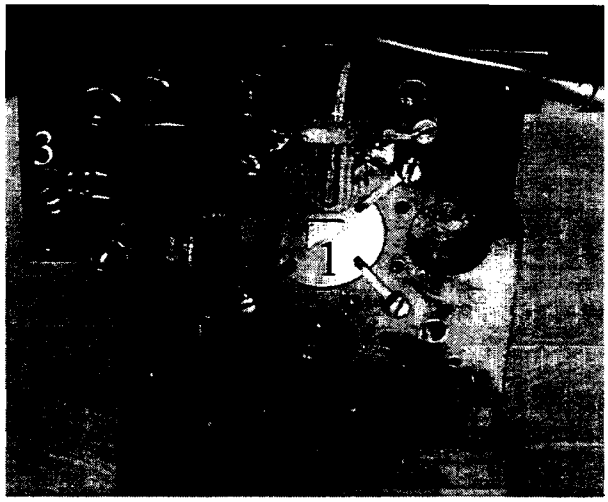

Figure 5: *Photograph of the mixer block. The lens and (h.l. broken) chip (1) and IF cable (2) can be clearly seen. Upper left is the thermometer (3). The connecting IF board (4) is also visible.*

5 RF Measurements

5.1 Receiver Setup

The on-chip HEB is placed in the second focus of a synthesized elliptical high-resistivity Si lens by gluing it to the lens. Instead of using beeswax we now use superglue. This is done to avoid damaging the bridge by heating it to melt the wax ($\sim$ 80°C).

Before applying glue, we align the antenna to the optical axis (accuracy better than 5 μm) by moving the die with micrometers to the center of the lens. Using a microscope with XY-table, this center is found relative to the lens' outer edge, which is accurately machined.

The lens itself is held in a copper block as can be seen in Fig. 5. To obtain good thermal contact, 4 springs press the lens softly into the In foil between the flange of the lens and the Cu block.

We find the temperature of the lens to be 4.7 K, not pumping the He-bath. The block is bolted to the cold plate, applying a small amount of Apiezon N vacuum grease for thermal contact. Connection to a standard

IF-chain[1] (centered at 1.4 GHz) is made by wire bonding to a microstrip line on a printed circuit board (Duroid^{TM}, 0.5mm thick, $\varepsilon_r = 4.7$), having < -10 dB reflection over a bandwidth of 4.7 GHz. A standard SMA-connector is soldered to its end to connect to the IF chain.

The window of our dewar is made of 195μm Mylar. Behind that, a black polyethylene IR-filter (105μm)is placed.

Y-factor measurements are done using a carcinotron or, in the near future, an FIR laser as a Local Oscillator (LO) source. A standard hot/cold setup (300 K/77 K) is used as a calibrated source, the signals of both being combined by a Mylar beam splitter (15μm).

5.2 RF Response Measurements

To characterize the RF response of the HEBMs, we use a Fourier Transform Spectrometer (FTS) to measure the relative coupling efficiency as a function of frequency. In doing these measurements, the device is kept at a temperature of about 4.8 K. A bias point slightly above the drop-back point is chosen to have optimal signal. In this paper, we show results for devices designed for both 1 THz and 2.5 THz. The data we show are obtained from 1 specific device, although similar data are measured on several devices.

Relative coupling efficiency for 1 THz devices shows good agreement with the predictions by the model sketched in section 2. The vertical scale of the FTS data is adjusted to give the best match to the simulation. As can be seen in Fig. 6 (solid line), a downward shift of about 12% from design value (1 THz) is observed. This can be well accounted for by taking actual device parameters into account (dashed line): the 500 nm line widths needed in the CPW turn out slightly wider (800 nm) in the fabrication process and R_{HEB} is 50% higher than designed.

The fact that we do not observe the increase in the measurements (starting around 1.3 THz) is due to the decrease of the main beam efficiency when off-center. Radiation is coupled into this main beam, so the observed efficiency goes down with respect to calculation. Optimization is done for the first peak only.

The 2.5 THz device on the contrary, shows its peak response over a wide band around 1.5 THz (solid line), a decrease of $\sim$ 30% with respect to the

[1]The IF chain consists of a Berkshire cryo-amplifier (44dB), an isolator, room temperature amplifier (44dB), band pass filter (80 MHz at 1.4 GHz) and a Hewlett Packard power meter. The total gain is 76dB.

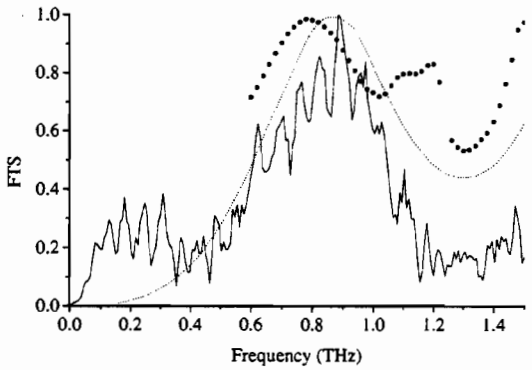

Figure 6: *FTS results and simulations on 1 THz-device. The solid curve is the measurement, the dotted curve is the analytical simulation. The solid dots are the distributed calculation with* $R_{HEB} = 51\Omega$. *See the text of section 6.*

curve that is simulated based on actual device geometry (Fig. 7, dotted). A similar, though not as severe, shift is observed by Karasik et al.[1]. Calculating the expected response based on actual device parameters results in a center frequency of 2.1 THz (dashed line). The observed and calculated bandwidth are in reasonable agreement.

5.3 Heterodyne measurements

Using a standard hot/cold technique we performed heterodyne measurements on a 1 THz bolometer. We determine the corrected receiver noise temperature to be 3600 K at an estimated bath temperature of 3.3 K and an IF-bandwidth of 1.25 GHz. The correction is for the beam splitter only.

Using the isothermal technique at relatively high V_{bias}, we find that about 40 nW of LO power is needed to obtain the highest Y-factor.

Fig. 8 shows the IV-curve of the pumped and unpumped device. The Y-factor does not change noticeably with varying LO frequency in the range of 0.90-0.94 THz. The IF bandwidth of the mixer is limited by the IF chain used (1.7 GHz).

The IV-curve of the device is fit using the hot spot model by Wilms Floet et al.[13]. This model describes the mixing in terms of a hot spot oscillating at IF. The IV-curves can be predicted using this model. Our experimental

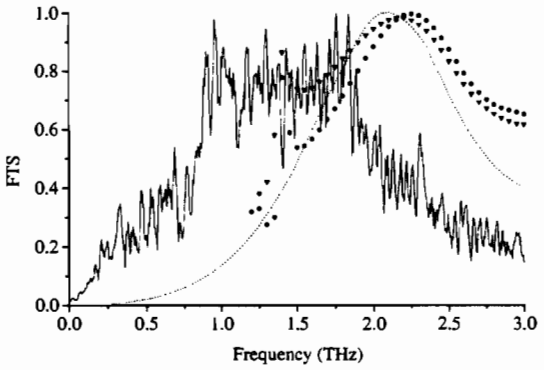

Figure 7: *FTS results and simulations on 2.5 THz-device. For* Z_{HEB} *the measured value* $R_{HEB} = 51\Omega$ *is taken. The solid curve is the measurement, the dotted curve is the analytical simulation. The solid dots are the distributed calculation with infinite* $\sigma_{groundplane}$*, the open dots assume* $\sigma_{groundplane} = 4.1 \times 10^7 \Omega m^{-1}$.

data can be well described by this model using realistic values for the relevant parameters in the model. For the LO power needed, we find 55 nW. This value agrees with the 40 nW obtained in the isotherm method, where it is assumed that absorption of DC power is uniform over the microbridge and hence, less RF power is needed to sustain the same hot spot length.

6 Discussion

Heterodyne measurements done on a similar system[14], although using a doube dipole, yield $T_N = 1880$ K at 1.267 THz, measurements on a twin slot by [1] at 2.5 THz yield 2750 K. Waveguide devices[15] have shown a best noise temperature of 1100K at 0.70THz. We expect to be able to decrease the noise temperature by cooling the device to 2.2K. Based on the decrease seen by[15], we expect a value in the order of 2500 K. A full noise breakdown has to be done in order to identify the major noise contributions.

As shown in the section on RF response measurements, devices designed for 1 THz have an RF response that can be well accounted for. Because the reason for the large difference between these devices and those designed for 2.5 THz is not clear, we investigate the origin of the additional shift in our

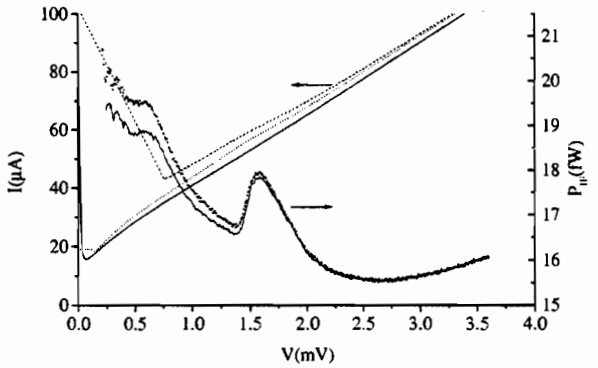

Figure 8: *Pumped (dotted) and unpumped (dashed) IV-curve of 1 THz device J1. The solid line is a simulation by the hot spot model. Hot (dots) and cold (line) IF output are also shown.*

2.5 THz geometry.

We do this by simulating the structure in a distributed element approach, in which we take into account the finite conductivity ($\sigma_{\text{groundplane}} = 4.1 \times 10^7\ \Omega^{-1}\text{m}^{-1}$) of the gold groundplane and the geometrical effect of the filter on the antenna. These calculations are done for both 1 THz and 2.5 THz.

The antenna-CPW-filter combination is drawn in Momentum[7]. At the position of the microbridge, a slot is assumed, keeping both CPW signal lines unconnected. To define a good plane of reference, a microstrip line with a via to the end of one CPW signal line is included. At the end of this microstrip line the reference plane is defined. It is checked that this microstrip line/via combination has little or no effect on the actual device. After calculation of the impedance at the position of the bolometer, the coupling of both impedances is calculated using equation 1 and the measured value for R_{HEB}.

Fig. 7 includes the results of a distributed element simulation on the designed structure compared to both measurement and an analytical simulation. It can be seen that the distributed element approach predicts the peak response frequency to be 10% lower than the original design (2.5 THz).

When the actual device geometry is put into the analytical simulations, peak response is expected at 2.1 THz. This is still 30% higher than the observed value.

To identify a possible cause for the shift, the influence of $\sigma_{\text{groundplane}}$ is looked at. It can be seen that including a finite groundplane conductivity ($\sigma_{\text{groundplane}} = 4.1 \times 10^7 \Omega^{-1}\text{m}^{-1}$, a reasonable value for our films) yields a small shift and also increases the band width. Including a finite groundplane conductivity still does not explain the large shift in response frequency.

We performed a similar analysis for the 1 THz device using the distributed element approach. Fig. 6 includes the results of a distributed element simulation on the designed structure compared to both measurement and an analytical simulation. The lumped (dotted) and distributed (solid dots) element-approach differ less than 10% in peak position, both their bandwidths agree with the measured bandwidth. Considering the fact that the actual CPW impedance, which is an important factor in the lumped-element peak position, is only roughly known, agree reasonably well in all three curves. The shoulder around 1.2THz is believed to be caused by structures present in the ground plane, e.g. the filter or filter-IF line transition.

To get rid of the structures in the CPW groundplane (i.e. filter, CPW transmission line) that may influence the antenna performance, we designed and produced a microstrip line design[16]. In that design, filter and antenna-bridge transmission line are included in the top layer of an $Al/SiO_2/Al$ microstrip line.

There are various reasons why we prefer the microstrip line design to the CPW. First, in a CPW-design, there is the already mentioned influence on the antenna properties. This is absent in the microstrip line design. Second, the microstrip transmission line has proven to work very well in an SIS-mixer up to 1 THz[17],[18]. Third, it allows us a much larger variation in characteristic impedance of the transmission line, making it easy to match a diffusion cooled HEB, which usually has a low impedance. Lastly, with respect to the fabrication, the microstrip line design is easier than that of the CPW transmission line because the structures can be defined by conventional optical lithography without the need of a high-resolution lithography such as e-beam lithography[1].

7 Conclusions

We report the design and fabrication of our quasi-optically coupled HEBMs for use at 1 and 2.5 THz. A twin slot antenna is used, in which the signal is transferred to the microbridge using CPW transmission lines.

The fabrication process for these devices is shown to work well. FTS measurements show the relative coupling efficiency to be in good agreement with the expected curve for 1 THz devices. For devices designed for 2.5 THz, a considerable down shift in peak response is observed. This shift cannot be accounted for in a more sophisticated approach based on the field distribution in the structure.

Our preliminary heterodyne measurements show a noise temperature of 3600 K at 0.93 THz. The IF bandwidth of the receiver is limited by the IF chain used.

8 Acknowledgment

Useful discussions with B. Jackson, H. Golstein, D. Van Nguyen, W. Laauwen and A. Baryshev and their support are acknowledged. This work is financially supported by the Stichting voor Technische Wetenschappen, which is part of the Nederlandse Organisatie voor Wetenschappelijk Onderzoek and partly by ESA under contract no. 11738/95/NL/PB.

References

[1] B.S. Karasik, M.C. Gaidis, W.R. McGrath, B. Bumble, and H.G. LeDuc. *IEEE Transactions on Applied Superconductivity*, 7:3580, 1997.

[2] S.S. Gearhart and G.M. Rebeiz. *IEEE Transactions on Microwave Theory and Techniques*, 42:2504–2511, 1994.

[3] Brian C. Wadell. *Transmission Line Design Handbook.* Artech House, Inc., 685 Canton Street Norwood, MA 02062, 1991.

[4] J. Zmuidzinas and H.G. LeDuc. *IEEE Transactions on Microwave Theory and Techniques*, 40:1797, 1992.

[5] M. Kominami, D.M. Pozar, and D.H. Schaubert. *IEEE Transactions on Antennas and Propagation*, 33:600, 1985.

[6] R. van der Laan. Master's thesis, University of Groningen, 1997.

[7] Hewlett Packard Advanced Design Software, Momentum planar solver.

[8] Sonnet EM software.

[9] D. Wilms Floet, J.J.A. Baselmans, J.R. Gao, and T.M. Klapwijk. Proceedings of the 9^{th} International Symposium on Space Terahertz Technology, Pasadena, CA. 1998.

[10] P.J. Burke, R.J. Schoelkopf, D.E. Prober, A. Skalare, M.C. Karasik, B.S. Gaidis, W.R. McGrath, B. Bumble, and H.G. LeDuc. *Journal of Applied Physics*, 85(3):1644, 1653 1999.

[11] D. Wilms Floet, J.J.A. Baselmans, T.M. Klapwijk, and J.R. Gao. *Applied Physics Letters*, 73(19):2826–2828, 1998.

[12] A. Skalare, W.R. McGrath, B. Bumble, H.G. LeDuc, P.J. Burke, A.A. Verheijen, R.J. Schoelkopf, and D.E. Prober. *Applied Physics Letters*, 68(11):1558–1560, 1996.

[13] D. Wilms Floet, E. Miedema, T.M. Klapwijk, and J.R. Gao. *Applied Physics Letters*, 74(3):433–435, 1999.

[14] A. Skalare, W.R. McGrath, B. Bumble, and H.G. LeDuc. *IEEE Transactions on Applied Superconductivity*, 7:3296, 1997.

[15] D. Wilms Floet, J.R. Gao, W.F.M. Ganzevles, T.M. Klapwijk, G. de Lange, and P.A.J. de Korte. Proceedings of the 10^{th} International Symposium on Space Terahertz Technology, Charlottesville, VA. 1999.

[16] W.F.M. Ganzevles, J.R. Gao, N.D. Whyborn, P.A.J. de Korte, and T.M. Klapwijk. page 504, 1998.

[17] M. Bin, M.C. Gaidis, J. Zmuidzinas, T.G. Phillips, and H.G. LeDuc. *Applied Physics Letters*, 68:1714, 1996.

[18] P. Dieleman, T.M. Klapwijk, J.R. Gao, and H. van de Stadt. *IEEE Transactions on Applied Superconductivity*, 7:2566, 1997.